Evaluation of MP2, DFT, and DFT-D Methods for the Prediction of Infrared Spectra of Peptides

Yves Bouteiller, Jean Christophe Poully, Charles Desfrançois, and Gilles Grégoire*

Laboratoire de Physique des Lasers, CNRS, UMR 7538, Institut Galilée, Université Paris 13, 93430, Villetaneuse, France

Received: February 20, 2009; Revised Manuscript Received: April 18, 2009

The prediction accuracy of second-order Moller−Plesset theory MP2 and density functional theory DFT-(D) with and without empirical dispersion correction within the resolution of identity approximation (ri) have been investigated for the assignment of infrared spectra of gas-phase peptides. A training set of 17 conformers of phenylalanine containing capped peptides have been used to establish mode-specific local scaling factors. Inclusion of dispersion terms at the DFT level turns to significantly improve the accuracy of predicted IR spectra. At the DFT-D level, the nonhybrid generalized gradient approximation functional B97-D (TZVP basis set) provides even better results than the popular hybrid functional B3LYP (6-31+G* basis set) while reducing the computational cost by almost 1 order of magnitude. Besides, MP2 (SVP basis set) outperforms all other tested methods in terms of reliability and transferability to larger molecular systems with typical prediction errors of about 5 cm^{-1}.

Introduction

In the past decade, a tremendous number of gas-phase experimental studies have been undertaken by means of double resonance IR/UV spectroscopy on isolated short peptide chains.[1] Single protected[2,3] and unprotected[4,5] amino acids, unprotected peptides,[6−9] β-sheet models,[10−12] β-turn,[13] γ-turn models,[14,15] and helical peptides[16,17] have been experimentally investigated mostly in the amide A region. With the advance of tunable narrow-band IR tabletop laser extending the spectral range down to 6−10 μm,[18,19] and the use of IR free electron laser,[20−23] infrared signatures of carbonyl stretch and NH bending modes can also be monitored. These gas-phase studies have provided a precise insight into the atomic interactions that govern the emergence of secondary structures in peptide model systems. One of the unique advantages of this experimental technique is to probe the local intramolecular interactions in a solvent-free environment or in a nanosolvated medium.[24−26] The molecules are cooled down in a supersonic expansion of rare gas atoms to ensure that only the lowest-energy isomers are significantly populated and investigated at low rovibrational temperatures. Conformer-selective IR spectra are thus recorded with a precision of a few wavenumbers and can be directly compared to quantum chemistry calculations to assert the structure of those molecules. The basis picture becomes a little more intricate when looking to larger peptides that exhibit less-resolved spectroscopic features[20,27,28] and for which high-level calculations are unaffordable.

Gas-phase structures of small peptide chains are mostly influenced by local intramolecular interactions. Electrostatic force plays a major role in the structure of biological molecules through the formation of hydrogen bonds between functional groups, N−H and C═O of the peptide bond, NH_2 amino group at the N terminal part, and carboxylic acid at the C terminal end of the peptide chain. In the above-mentioned experimental studies, the peptides possess an aromatic residue in which the chromophore bears the oscillator strength for UV excitation. With aromatic residue containing peptides, dispersion forces are not negligible especially for structures showing a strong NH−π interaction. It has been shown that, for capped dipeptides, a minor interaction like NH−π is capable of forcing the molecules to adopt a certain conformation stabilized by local interactions, like C_5 and C_7, instead of forming a folded structure through a C_{10} H-bond along the backbone chain.[29] These subtle types of interactions are responsible for stabilizing in a large propensity β-strand (β_L) and γ-turn (γ_L) conformations in small dipeptides, whereas secondary structures like β-turn, 3_{10}, and α helices emerge in tripeptides and coexist with these local conformational preferences. Because the structure of gas-phase peptides is strongly influenced by a variety of interactions, conformer assignment requires high-quality theoretical methods.

Among the theoretical methods, DFT-based calculations, due to their reasonable computational costs and rather reliable results, are the most popular ones to predict the structure through comparison between predicted and experimental IR spectra. However, DFT method generally fails to properly describe strong intermolecular H-bond interactions, as the ones encountered in the hydrates[30−33] and dispersion-bound systems.[34] This last drawback relies on the inability to describe electron correlation effects at the DFT level with standard functionals. Recently, two different approaches were adopted to cover the dispersion energy missing at the DFT level. Truhlar and coworker have developed new functionals M05−2X[35] and M06−2X[36] parametrized to properly account for noncovalent interactions such as aromatic stacking. In a second approach, the dispersion energy is explicitly added to the DFT energy by a damped pair-potential empirical term.[37,38] DFT augmented with an empirical dispersion term, noted DFT-D, has been introduced as a promising method for correctly describing biomolecular systems where dispersion interaction is not negligible.[39] Nonhybrid GGA functionals have been found to provide good agreement in terms of structural parameters and relative energy of biomolecules with the high-level CCSD(T) method although saving considerable computational time.[40−42] Whereas high-level

* To whom correspondence should be addressed. E-mail: gilles.gregoire@univ-paris13.fr.

10.1021/jp901570r CCC: $40.75
Published on Web 05/12/2009

correlated ab initio methods (like CCSD(T)) can effectively account for the structure and energetic of molecules, their uses are strictly limited to small-size systems.

The second-order Moller−Plesset perturbation theory (MP2) may offer a good alternative to treat medium-size systems, with regard to its computer time saving while describing in a moderated way electron correlation. Besides, the resolution of identity (ri) approximation, which reduces the computational time by roughly 1 order of magnitude, has been shown to marginally differ from exact calculations.[43,44] In most of the theoretical studies, MP2 methods have been evaluated by looking at structural parameters and interaction energies in comparison with more elaborate but time-consuming ab initio theories.[45] Hobza and co-workers have documented the competition between H-bond and π-stacking interactions in nucleic acid base systems[46−49] and also studied the influence of these interactions in the structural properties of aromatic amino acid-containing peptides.[50,51] However, much less attention has been paid to the prediction of the vibrational frequencies at the MP2 level,[52−54] although being the only experimental observable that can be measured with a high precision, in regard to the predicted accuracy expected for the different theoretical methods.

Theoretical DFT and ab initio studies support the experimental works in particular in the vibrational analysis but these studies are generally limited to the simple harmonic approach known to provide an approximate description requiring the use of a scaling factor to obtain the vibrational frequencies. Two different methods, the vibrational self-consistent field (VSCF) and the second order perturbative vibrational traitement (PT2), have been devised for taking into account the problem of the anharmonicity of vibrational modes. These methods have been applied with success to small molecules[55,56] and molecular systems of biological interest, like DNA bases,[57] amino acids,[58] and small peptides.[59] Although fundamental vibrational bands can be assigned without any scaling factor and maximum errors similar to the ones obtained through scaled harmonic approximation,[60] their uses are most usually limited to rather-small-size molecules with less than few tens of atoms. On the other hand, scaling factors must be applied to harmonic frequencies to take into account the discarded anharmonicity terms. We have recently proposed a set of transferable scaling factors for assignment of IR spectra of gas-phase biomolecules,[61] including nucleobases, amino acids, peptides, sugars, and neurotransmitters, at the DFT B3LYP and B3PW91 level for different basis sets ranging from 3−21G up to 6-311++G**. We have concluded that the best compromise in terms of accuracy and computational time is obtained with the 6-31+G* basis set, which leads to frequency prediction on average within 10 cm^{-1} (in the range of 3700−1500 cm^{-1}), whereas the use of a larger basis set like 6-311++G** does not yield much better results.

In this present work, we have thus focused our investigation to rather small- or medium-size basis sets with the goal of using these methods for large peptides that are now experimentally studied. The aim of this study is thus to establish the degree of confidence and transferability that one might expect from the prediction of IR spectra of gas-phase peptides. We report on the vibrational frequency analysis at the MP2, DFT/B3LYP, and DFTD/(B3LYP, BLYP and B97-D) levels for 17 conformations of protected peptides containing a phenylalanine residue that have been studied by means of double resonance IR/UV spectroscopy.[29] We will compare the precision of the predicted frequency following the determination of specific local scaling factors for NH_2 asymmetric and symmetric, NH, CO stretches, NH_2, and NH in-plane bending (ipb) modes. We will further look at the dependence of the amide A band as a function of the type of interactions, namely NH-C_5, π, and C_7 that are responsible for the conformational preferences of short peptide chains in the gas phase. We finally illustrate on three alanine containing capped tripeptides the efficiency of the MP2 method to predict their IR spectra in which π, C_5, C_7, and C_{10} interactions are encountered.

Methods

A training set of 17 conformers of capped peptides, Ac-Phe-NH_2, Ac-Phe-Xxx-NH_2 and Ac-Xxx-Phe-NH_2 (Xxx = Gly, Ala, Val, and Pro) that have already been studied and well characterized has been used in this study to deduce the specific scaling factors of the investigated vibrational modes. The list of the peptides and their different conformations is reported as Supporting Information. All of the calculations have been performed with the *Turbomole v5.10* program package.[62] Correlated quantum chemistry calculations have been performed at the MP2 level using the approximate resolution of identity (ri) methods[63] together with two Ahlrichs atomic basis sets, namely VDZ (noted SVP in Turbomole)[64] and TZVP,[65] the Dunning cc-pVDZ basis set[66] and their corresponding ri-auxiliary basis sets.[67,68] We have checked on some molecules that the ri approximation at the MP2 level does not change the calculated frequency by more than 1−2 cm^{-1} as compared to the exact calculation. DFT and DFT-D calculations have been performed using the B3LYP hybrid generalized gradient approximation (GGA) functional[69,70] again within the ri approximation together with Ahlrichs VDZ (noted def2-SVP in *Turbomole*)[64] and its ri-auxiliary basis set[71] and Pople 6-31+G* basis sets.[72] We add the 6-31+G* basis set in this study because it is the one that has been widely used in previous works together with the DFT/B3LYP method and which gives rather reliable results so far.[61] Because the *Turbomole* package does not include a 6-31+G* auxiliary basis set needed for ri approximation, we have used Ahlrichs VDZ (def2-SVP)[71] as an auxiliary basis set. To test its validity, we have compared the predicted frequency of some conformers at the DFT B3LYP/6-31+G* with and without the ri approximation and found similar values within less than 2 cm^{-1}. Note that the B3LYP functional implemented in *Turbomole* slightly differ from the one implemented in the *Gaussian* package.[73] The empirical dispersion correction of Grimme for DFT-D calculations has been used as implemented in *Turbomole*.[37] Besides, we have tested the B-LYP[69] and B97-D[40] nonhybrid GGA functionals at the ri-DFT-D level. Although BLYP and more generally nonhybrid functionals are known to underestimate X−H frequencies,[74] these fonctionals have been chosen because they lead to significant computer time saving as compared to the hybrid B3LYP functional. These two functionals have been tested along with the 6-31+G* basis set and the triple-ζ TZVP basis set.[65,75]

All of the ri-MP2 calculations have been done using the parallel version of *Turbomole*,[76] whereas the ri-DFT B3LYP and ri-DFT-D parallelized calculations are not yet implemented. Harmonic vibrational frequencies have been calculated numerically for all methods. Calculations have been performed on a 16 nodes dual processor PC cluster (Alineos) with 2GB of RAM per CPU.

For each level of theory L (ri-MP2, ri-DFT, ri-DFT-D, and basis set) and each of the vibrational modes υ, individual scaling factors $a_{scal}^{i,j,\upsilon,L}$ have been simply obtained by dividing the experimental value $\nu_{exp}^{i,j,\upsilon}$ published in the literature for a molecule i in a given conformation j by the corresponding calculated value $\nu_{cal}^{i,j,\upsilon,L}$. The here proposed gas-phase transferable specific scaling

factors $a_{scal}^{v,L}$ have then to be obtained by simple arithmetic averaging of the individual values deduced from the training set of molecules. The predicted frequency values are, by definition, equal to $\nu_{predict}^{i,j,v,L} = a_{scal}^{v,L}\,\nu_{cal}^{i,j,v,L}$. To evaluate the prediction capabilities and the transferability of those scaling factors, we also calculate the average of the errors between predicted and experimental frequency $\varepsilon_{v,L} = (\sum \nu_{predict}^{i,j,v,L} - \nu_{exp}^{i,j,v})/(n)$ and the standard deviation $\sigma_{v,L}^2$ given by $\sigma_{v,L}^2 = (n\sum(\nu_{predict}^{i,j,v,L} - \nu_{exp}^{i,j,v})^2 - (\sum(\nu_{predict}^{i,j,v,L} - \nu_{exp}^{i,j,v})))/(n(n-1))^2$, n being the number of investigated vibrational modes. As mentioned above, because the exact (non-ri) and resolution of identity approximation methods lead to similar frequency calculations within less than 2 cm^{-1}, it is assumed that the proposed scaling factor for predicting the IR spectrum of gas-phase peptide can be used even for the exact (non-ri) MP2 and DFT-(D) methods. In any case, the ri approximation introduces negligible errors as compared to all other sources of error inherent of the methods, functionals, and limited-size basis sets.

Results and Discussion

The training set used to calculate the local scaling factors is chosen among selected conformers of protected phenylalanine- and phenylalanine-containing protected dipeptides. Seventeen conformations have been theoretically investigated following the experimental study of M. Mons et al. recently reported in a review article.[29] IR spectroscopy of the peptides have been achieved with a narrow-band IR OPO laser in the amide A region, the experimental resolution being 1 cm^{-1}, whereas the amide I and II regions (1500−1700 cm^{-1}) have been investigated with the IR free electron laser (FELIX, Netherlands) with a lower spectral resolution, about 10 cm^{-1}, which leads to a larger experimental uncertainty in the band positions. A systematic investigation of the effect of the nature and position of the residues has led to a refined methodological approach to probe the local intramolecular interactions, in particular the H-bonding schemes. First-order assignments have thus been proposed following the conformational landscape of the peptide backbone, that is, β_L, γ_L, and β-turn. For Ac-Phe-Xxx-NH_2, structure assignments have been confirmed through comparison with B3LYP/6-31+G* calculations,[15] whereas for Ac-Xxx-Phe-NH_2, calculations have only been performed for the glycine residue.[21]

In the present study, we have further investigated the possible conformations of the dipeptides to unambiguously assign their IR spectra. Exploration of the potential-energy surface is conducted at the AM1 level (hyperchem), and fully optimized at the ri-MP2/SVP level. For each of the low-energy conformers within 3 kcal/mol above the absolute minimum, the predicted IR spectrum has then been calculated and compared to the experimental one. In all cases, the best agreement is found for the most stable conformer (E+ZPE), which has led to a precise conformer assignment for all of the studied peptides including the chirality *L/D* and the side-chain orientation (a, g+, g-) for both residues. We first report on the ri-MP2 and B3LYP ri-DFT-(D) calculations to easily compare the efficiency of these methods and to analyze the effect of the dispersion correction at the DFT level, whereas the results for the nonhybrid GGA functionals ri-DFT-D calculations will be presented at the end of the manuscript.

The local scaling factors for NH_2 (asymmetric and symmetric), NH, and CO stretches and NH_2 and NH in-plane bending (ipb) modes have been obtained on a set of 34, 20, 29, 11, and 18 experimental values, respectively. The local scaling factors are reported in Table 1 for the different level of theory and basis set used. The standard deviation $\sigma_{v,L}$ are reported in Table 2 for the three basis sets used with the ri-MP2 method and for the two basis sets at the B3LYP ri-DFT and ri-DFT-D levels.

TABLE 1: Local Scaling Factor for the ri-MP2 and B3LYP/ri-DFT and ri-DFT-D Methods

	ri-MP2			ri-DFT/B3LYP		ri-DFT-D/B3LYP	
	SVP	TZVP	cc-pVDZ	SVP	6-31+G*	SVP	6-31+G*
NH_2	0.9409	0.9487	0.9491	0.9627	0.9603	0.9668	0.9638
NH	0.9412	0.9476	0.9485	0.9567	0.9561	0.9580	0.9570
CO	0.9415	0.9738	0.9572	0.9567	0.9787	0.9557	0.9774
NH_2 ipb	0.9794	0.9713	0.9846	0.9975	0.9672	0.9939	0.9654
NH ipb	0.9568	0.9699	0.9694	0.9772	0.9709	0.9698	0.9623

TABLE 2: Standard Deviation for ri-MP2 and B3LYP/ri-DFT and ri-DFT-D Methods; All Values in cm^{-1}

	ri-MP2			ri-DFT/B3LYP		ri-DFT-D/B3LYP	
	SVP	TZVP	cc-pVDZ	SVP	6-31+G*	SVP	6-31+G*
NH_2	7.8	7.2	12.2	12.5	4.5	18.6	7.6
NH	5.9	12.6	6.3	13.5	15.5	14.4	9.4
CO	5.8	4.8	6.3	7.9	5.1	7.3	4.3
NH_2 ipb	3.9	3.7	5.0	4.2	3.1	6.0	5.8
NH ipb	5.5	6.5	6.0	5.1	5.2	8.0	7.6

In overall, the standard deviations for the CO stretch, NH_2, and NH ipb modes are below 8 cm^{-1}, whereas the NH_2 and NH stretches show much larger deviations up to 15 cm^{-1}. The asymmetric and symmetric NH_2 stretches are indeed systematically over and underestimated respectively, as revealed by the positive and negative values of $\epsilon_{v,L}$ (Table S1 of the Supporting Information). This trend is however less prominent at the ri-MP2/TZVP and ri-DFT/B3LYP/6-31+G* levels. This clearly points to a specific behavior of the NH_2 stretches for the asymmetric and symmetric modes. These modes (3300−3550 cm^{-1}) can be in Fermi resonances with amide I (1700 cm^{-1}) and NH_2 ipb modes (1600 cm^{-1}) and can be influenced differently.[59] As previously reported,[61] the prediction performances are significantly improved when introducing a specific scaling factor for the two NH_2 stretches. These specific local scaling factors for asymmetric and symmetric NH_2 stretches are reported in Table S2 of the Supporting Information. In the following, the analysis of the NH_2 stretching modes according to the type of interactions has been obtained with these specific scaling factors. For the NH stretch, the standard deviations are significantly larger at the ri-DFT/B3LYP level for the two basis sets used than at the ri-MP2 level, only the TZVP basis set giving a rather poor results at the ri-MP2 level. Because the largest errors are found for the NH stretch modes, we have further looked at the accuracy of the predicted calculations for the different types of interactions, namely NH−C_5, π, and C_7 encountered respectively 6, 9, and 4 times in the peptide training set. Because NH_2−C_7- and C_{10}-type of interactions, present 11 and 5 times in the training set, which compete with the above-mentioned local interactions, are responsible for the formation of folded secondary structures in these peptides, they have also been carefully checked. The average of the errors and the corresponding standard deviations for the predicted frequencies are reported in Table 3 for ri-MP2 and for B3LYP/ri-DFT and ri-DFT-D methods. In most of the cases, for each H bond motif the errors from the experimental value are of same sign, that is either blue- or red-shifted. This is reflected in the non-null mean error values with reduced standard deviation compared to the global ones reported in Table 2.

TABLE 3: Average of the Error ε and Standard Deviation (in Parentheses) for the Different H-Bond Interactions for ri-MP2 and B3LYP/ri-DFT and ri-DFT-D Methods; All Values in cm^{-1}

	ri-MP2			ri-DFT/B3LYP		ri-DFT-D/B3LYP	
	SVP	TZVP	cc-pVDZ	SVP	6-31+G*	SVP	6-31+G*
NH−C_5	3.0(3.4)	8.6(5.3)	2.5(4.7)	−14.2(4.6)	−17.0(2.7)	−4.8(2.1)	−8.0(2.6)
NH−π	−4.1(3.0)	−11.2(5.6)	−4.4(2.5)	12.7(6.9)	2.8(5.4)	12.3(7.9)	4.0(7.2)
NH−C_7	7.2(0.3)	12.2(12.1)	8.4(1.6)	−4.5(6.4)	22.8(7.0)	−18.2(14.1)	6.1(11.2)
NH_2^{as}−C_7[a]	−1.7(4.2)	−1.5(5.1)	−4.3(7.3)	−0.7(3.2)	−0.9(3.6)	0.0(1.8)	−0.1(2.0)
NH_2^{s}−C_7[a]	0.4(5.4)	3.1(7.2)	−3.0(6.1)	−2.8(7.1)	1.2(5.1)	0.0(5.8)	3.0(6.5)
NH_2^{as}−C_{10}[a]	3.5(1.8)	6.5(4.1)	10.3(8.7)	−0.5(2.9)	1.7(3.0)	−2.2(1.9)	0.3(2.6)
NH_2^{s}-C_{10}[a]	0.4(1.3)	−2.1(1.4)	9.2(6.1)	2.2(9.3)	−2.6(6.2)	−5.0(6.4)	−7.3(3.5)

[a] Calculated with the specific local scaling factors for asymmetric and symmetric NH_2 stretches.

At the ri-MP2 level, both SVP and cc-pVDZ basis sets give similar errors for the NH stretching modes, slightly underestimate C_5 and C_7 interactions while overestimate the NH−π interactions. Interestingly, the larger basis-set TZVP enhances these trends although we would expect a better accuracy as compared to the smaller basis set used in this study. In particular, the NH−π interaction is poorly described by a systematic red shift of the predicted frequency of −11 cm^{-1} on average, more than two times larger than the red shift found with the SVP basis set. This could be related to the inherent trend of the MP2 method to overestimate the binding in dispersion-bound systems, which might be more pronounced as the size of the basis set increases.[45,77] Nevertheless, it is noteworthy that although the experimental frequencies of the NH modes engaged in such different C_5 and C_7 patterns spanning over 200 cm^{-1}, ri-MP2 methods predict them within 10 cm^{-1}, the SVP basis set giving the best accuracy with the lower standard deviation below 5 cm^{-1}. Besides, the NH_2 stretches engaged in C_7 and C_{10} types of interactions are very well reproduced at the ri-MP2 level for the Ahlrichs basis sets, SVP being here again slightly better than TZVP, whereas the Dunning cc-pVDZ basis set leads to larger errors and standard deviations.

At the ri-DFT/B3LYP level, NH_2 stretches are satisfyingly predicted as reported in Table 3, with mean errors similar to the ones found at the ri-MP2 level. However, both SVP and 6-31$^+$G* basis sets fail to correctly simulate the NH stretches involved in the different types of H bonding. First, a weak H-bond like that in the C_5 pattern is systematically overestimated by about 15 cm^{-1}. For the two other H-bond motifs, NH−π and C_7, the results are basis-set dependent. At the SVP level, a satisfying agreement is found for the NH−C_7 frequency with an average red shift of 4.5 cm^{-1}, whereas NH−π frequencies are on average strongly blue-shifted by 13 cm^{-1}. Conversely, at the 6-31+G* level, strong H-bond interactions like those encountered in a C_7 pattern are systematically underestimated by more than 20 cm^{-1}. For instance, in Ac-Pro-Phe-NH_2−$\gamma_L\gamma_L$(g-), the experimental frequency lies at 3261 cm^{-1},[14] red-shifted by about 200 cm^{-1} from the free NH, and is predicted at 3296 cm^{-1} at the ri-DFT/B3LYP/6-31$^+$G* level, leading to a 35 cm^{-1} blue shift of the predicted band. Because dispersion is not properly described at this level of theory, one would expect a larger error in the predicted NH−π frequencies as compared to the C_5 ones. The inverse is clearly observed and might be due to the compensation of errors. This can be qualitatively explained by looking at the structural property of peptides in a $\beta_L\gamma_L$ conformation, which exhibits both C_5 and π types of interaction. In part a of Figure 1, comparison of the structural motifs in $\beta_L\gamma_L$ conformation of Ac-Phe-Ala-NH_2 between ri-MP2/SVP and ri-DFT/B3LYP/6-31+G* clearly revealed the influence of the poor description of the π interaction in this system, with a larger NH−π distance at the DFT level

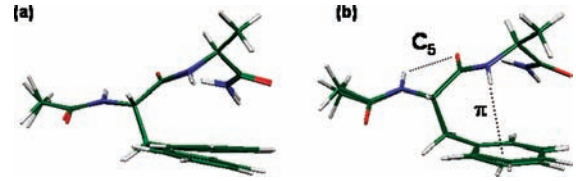

Figure 1. Superimposed structures of AcPheAla_β_L(a)γ_L following the different methods of calculation; (a) comparison between ri-MP2/SVP level (benzene ring perpendicular to the plane) and ri-DFT/B3LYP/6-31+G* level in which the benzene ring adopts an opened structure, (b) ri-DFT-D/B3LYP/6-31+G* and ri-MP2/SVP lead to very similar structures.

and a corresponding extra stabilization of the C_5 bonding revealed by the slightly shorter interatomic NH−O distance (2.22 vs 2.17 Å respectively). The concomitant red shift and blue shift of the closely C_5 and NH−π frequencies leads to a systematic inversion in their order at the DFT level for the two basis sets used in this study. For instance, the experimental splitting of the two C_5 and π amide A bands is +23 cm^{-1} for Ac-Phe-Ala-NH_2 in the $\beta_L(a)\gamma_L$ configuration,[15] which is well reproduced at the ri-MP2/SVP level (+31 cm^{-1}), whereas the predicted splitting is −11 and −4 cm^{-1} at the ri-DFT/B3LYP/SVP and 6-31+G* levels, respectively.

The performance of the DFT augmented with an empirical dispersion term (ri-DFT-D) has been evaluated both on the structures and frequencies analysis for the training set of peptides. The structures of the peptides at the ri-DFT-D/B3LYP level are very similar to the ones found at the ri-MP2 level, as illustrated in part b of Figure 1 for Ac-Phe-Ala-NH_2_$\beta_L(a)\gamma_L$ for which the peptide backbone is bent over the aromatic chromophore. This trend has already been noticed in previous studies, which has led to the conclusion that DFT-D methodology might offer a good compromise between accuracy and computational cost as compared to more sophisticated ab initio methods. However, only few studies have focused on the performance of the DFT-D method to simulate the IR spectra of peptides. Hobza et al. have reported that, using TPSS functional, the inclusion of the dispersion term (following their own implementation) does not affect by more than few wavenumbers the high-frequency modes as compared to those the normal DFT method.[41] It was then concluded that the DFT-D/TPSS method inherits the performance from pure DFT/TPSS calculation, although the accuracy for predicting the IR spectrum of such functional is sparsely documented. Besides, very few studies have been done so far for the most popular B3LYP functional.[78,79]

In overall, the performance of the ri-DFT-D/B3LYP method for predicting the IR spectra of the studied peptides is slightly better than without the inclusion of the dispersion term but strongly depends on the basis set used. As reported in Table 2,

TABLE 4: Local Scaling Factor for the ri-DFT-D/ B-LYP and B97-D Methods

	ri-DFT-D/B-LYP		ri-DFT-D/B97-D	
	TZVP	6-31+G*	TZVP	6-31+G*
NH_2	0.9976	0.9986	0.9812	0.9841
NH	0.9903	0.9914	0.9761	0.9790
CO	1.0283	1.0239	1.0072	1.0029
NH_2 ipb	1.0076	0.9984	0.9973	0.9862
NH ipb	1.0093	1.0004	0.9988	0.9881

TABLE 5: Standard Deviation σ for ri-DFT-D/ B-LYP and B97-D Methods; All Values in cm^{-1}

	ri-DFT-D/B-LYP		ri-DFT-D/B97-D	
	TZVP	6-31+G*	TZVP	6-31+G*
NH_2	18.1	15.4	14.0	12.4
NH	11.8	11.2	7.5	9.1
CO	5.3	5.2	5.2	5.0
NH_2 ipb	6.8	7.6	5.1	6.0
NH ipb	9.6	8.5	7.5	7.4

the standard deviations are larger at the SVP level. For the 6-31$^+$G* basis set, the performances are rather similar excepted for the NH stretch mode for which the standard deviation is significantly reduced. The analysis of the results for the different types of H-bond interactions is reported in Table 3. For the NH_2 stretches, both ri-DFT and ri-DFT-D methods give similar results for the two basis sets with a good agreement with the experimental values. For the NH stretching mode, the same trends are observed for the different types of interaction following the two basis sets. The H-bond strength is strongly reduced for C_5 interaction, strongly amplified for C_7 interaction, whereas no significant change is observed for the NH$-\pi$ interaction. At the SVP level, this leads to a lower error down to -5 cm^{-1} for C_5 interaction, while increasing the errors for the C_7 interactions to -18 cm^{-1}. For the 6-31$^+$G* basis set, π interaction is still well reproduced and the respective red shift (-17 cm^{-1}) and blue shift ($+25$ cm^{-1}) of the C_5 and C_7 interactions found at the ri-DFT level are significantly reduced down to -8 and $+6$ cm^{-1}. Whereas the order of the C_5 and π interactions is inverted at the ri-DFT/B3LYP level, the inclusion of the dispersion term corrects this error. It turns out that the ri-DFT-D/B3LYP method provides a rather satisfactory performance at the 6-31$^+$G* level but is not recommended with the SVP basis set. Although the mean errors for the different types of interactions at the ri-DFT-D/B3LYP/6-31+G* level become similar to the ones found at the ri-MP2/SVP level, their standard deviations are larger. One can thus expect that the ri-DFT-D/B3LYP/6-31+G* method might become less reliable compared to ri-MP2/SVP in terms of transferability.

Two nonhybrid GGA functionals, B-LYP and B97-D, have been tested at the ri-DFT-D level together with the 6-31+G* and the TZVP basis sets. The triple-ζ basis set has been chosen because SVP leads to even worse results than those for B3LYP/SVP. Besides, with the computer time saved by the ri approximation together with the use of nonhybrid functional, such a larger basis set can be used without a significant increase in computational time as compared to the 6-31+G* level. The local scaling factors for the probed modes are reported in Table 4, the standard deviations are reported in Table 5, and the errors and standard deviations in the prediction of the different type of H-bond interactions are reported in Table 6 for the two functionals and the two basis sets.

As it can be seen in Table 4, the scaling factors for the two nonhybrid GGA functionals are close to unity for all probed vibrations, excepted for the amide A mode with B97D. This is in straight contrast with the ones found with the B3LYP functional and at the MP2 level. The good agreement between unscaled harmonic frequencies and experimental data simply relies on error compensations, that is the neglect of anharmonicity is compensated by the underestimation of the harmonic frequencies.[55]

TABLE 6: Average of the Error ε and Standard Deviation (in Parentheses) for the Different H-Bond Interactions for ri-DFT-D/ B-LYP and B97-D methods; All Values in cm^{-1}

	ri-DFT-D/B-LYP		ri-DFT-D/B97-D	
	TZVP	6-31+G*	TZVP	6-31+G*
NH$-C_5$	$-1.7(1.6)$	$-3.2(2.4)$	$-2.6(1.4)$	$-6.0(2.2)$
NH$-\pi$	10.0(6.6)	9.1(8.1)	3.1(6.5)	3.3(8.3)
NH$-C_7$	$-17.2(6.6)$	$-11.9(9.5)$	0.4(11.9)	$-6.2(7.7)$
$NH_2^{as}-C_7$[a]	$-1.3(2.5)$	$-1.5(3.0)$	$-1.5(2.5)$	$-2.0(3.5)$
$NH_2^{s}-C_7$[a]	0.2(4.1)	0.1(5.4)	0.3(4.8)	$-0.5(7.0)$
$NH_2^{as}-C_{10}$[a]	2.2(2.0)	3.6(2.8)	4.0(2.4)	5.6(2.7)
NH_2^{s}-C_{10}[a]	$-4.8(4.8)$	$-1.5(3.1)$	$-1.6(5.0)$	0.7(1.0)

[a] Calculated with the specific local scaling factors for asymmetric and symmetric NH_2 stretches.

As already noted for the other methods, the asymmetric and symmetric NH_2 stretches are systematically under- and overestimated (Table S3 of the Supporting Information), which has led us to propose here again specific scaling factors for these two NH_2 stretches (Table S4 of the Supporting Information). As it can be seen in Tables 5 and 6, for a given basis set, B97-D performs better than B-LYP, with B97-D/TZVP giving the best results. For the NH_2 modes, the agreement is rather good for all methods, whereas the NH stretches exhibit large discrepancies between the two functionals. At the ri-DFT-D/BLYP level, only the C_5 type of interaction is satisfyingly simulated, whereas π and C_7 interactions are systematically under- and overestimated, respectively. B97-D leads to significantly better results, with errors ca. 6 cm^{-1}, TZVP leading to slightly better results than 6-31+G*. As already noticed with the B3LYP functional, the ri-DFT-D/B97-D/TZVP method gives the proper order for the strength of the weak NH$-C_5$ and π interactions. Interestingly, the performance of the ri-DFT-D/B97-D/TZVP method is similar and even slightly better than for the ri-DFT-D/B3LYP/6-31+G*. Besides, the computational time is greatly reduced when using nonhybrid functional. For Ac-Phe-Val-NH_2 (45 atoms), energy and gradient are calculated in less than 5 min at the B97D/TZVP level, whereas it takes more than 30 min with B3LYP/6-31+G*. Therefore, it could be advantageous to use the B97-D functional against the more popular B3LYP at the ri-DFT-D level. Compared to the ri-MP2/SVP method, while the mean errors for the different types of H-bond pattern are rather similar, the standard deviations are in general larger at the ri-DFT-D level, excepted for the NH$-C_5$ type of interactions. It is thus believed that its use for predicting IR spectra of larger peptides might be less reliable than that for ri-MP2. Although the computational cost for ri-MP2 is more than 1 order of magnitude larger than that at the ri-DFT-D level using nonhybrid GGA functionals, ri-MP2 calculations can be reasonably performed when using the parallel version of *Turbomole*. With the use of eight CPUs, ri-MP2/SVP calculations are only two times longer than that for ri-DFT/B97-D/TZVP.

We have tested the performance of the ri-MP2/SVP and ri-DFT-D/B97-D/TZVP methods on three capped tripeptides containing a phenylalanine residue for which IR spectra were previously recorded.[80] The IR assignments are reported in Table

TABLE 7: Experimental (Bold) and Calculated ri-MP2/SVP and ri-DFT-D/B97-D/TZVP IR Spectra of Ac-Phe-Ala-Ala-NH_2, Ac-Ala-Phe-Ala-NH_2, and Ac-Ala-Ala-Phe-NH_2 Capped Tripeptides

	NH_2^{as}	NH_2^{s}	NH_{i+1}	NH_{i+2}	NH_{i+3}
Ac-FAA-NH_2 β_L(a) γ_L γ_L[b]	**3522 C_7**	**3363 C_7**	**3447 C_5**	**3423 π**	**3338 C_7**
ri-MP2/SVP	3516	3360	3447	3414	3337
ri-DFT-D/B97-D/TZVP	3517	3361	3445	3424	3345
Ac-AFA-NH_2 3_{10}(g+)[b]	**3534 C_{10}**	**3408 C_{10}**	**(a) f**	3429 π	**3374C_{10}**
ri-MP2/SVP	3542	3412	3461	3422	3378
ri-DFT-D/B97-D/TZVP	3543	3426	3467	3429	3362
Ac-AAF-$NH_2\gamma_L$-βI(g+)[b]	**3524 C_{10}**	**3389 C_{10}**	**(a) f**	3303 C_7	**3440 π**
ri-MP2/SVP	3522	3387	3464	3314	3437
ri-DFT-D/B97-D/TZVP	3529	3396	3467	3285	3438

[a] missing NH stretch band located in the absorption region of the IR OPO laser [b] experimental values and conformer nomenclatures taken from ref.[68]

7 for Ac-Phe-Ala-Ala-NH_2, Ac-Ala-Phe-Ala-NH_2, and Ac-Ala-Ala-Phe-NH_2. At the ri-MP2/SVP level, all of the probed modes are predicted within 10 cm^{-1} or less, whatever the type of H-bond interactions, which clearly outperforms the other theoretical assignments, either at the DFT-D/B97-D/TZVP level which shows deviation up to 18 cm^{-1} or as previously reported at the DFT/B3LYP/6-31+G* level.[80]

Conclusions

We have compared the performances of the ri-MP2 and ri-DFT-(D)/B3LYP and ri-DFT-D/BLYP and B97-D methods for predicting the IR spectra in the amide A, I, and II regions of gas-phase small and medium size peptides. Seventeen conformations of capped peptides have been theoretically investigated leading to the determination of specific local scaling factors for the asymmetric and symmetric NH_2, NH, CO stretches and NH_2 and NH ipb modes. Overall, ri-MP2 provides more reliable results than ri-DFT for a comparable size of the basis set. The inclusion of an empirical dispersion term in the ri-DFT/B3LYP calculations leads to a significant improvement in the accuracy of the predicted frequencies only at the 6-31$^+$G* level. For the nonhybrid GGA functional within the ri-DFT-D method, B97-D gives more accurate results than BLYP for the two basis sets used. Besides, B97-D/TZVP can be recommended against B3LYP/6-31+G* due to its computational time saving and reliable results. Finally, the ri-MP2/SVP method provides the best agreement in terms of absolute accuracy and standard deviation. It is noteworthy that, at the ri-MP2 level, the use of a small basis set like SVP provides more reliable simulated IR spectra than with a larger basis set such as TZVP. Other studies have recently reported on the overestimation of stabilization energy at the MP2 level with increasing basis set.[45,77] It is clear that such a counterintuitive basis-set effect is based on compensation of errors on which we could not rely. Because balancing between inherent errors of the method and errors due to the truncated basis set, unless reaching the complete basis-set limit, will always occur, we thus might be cautious against the transferability to larger molecular systems. Nevertheless, the very satisfying simulated IR spectra of three capped tripeptides at the ri-MP2/SVP level using the local scaling factors deduced from the training set of smaller peptides indicates that this method can still be applied with confidence for molecules possessing at least 50 atoms. With the use of the proposed specific scaling factors, the IR spectrum can be simulated at the MP2/SVP level with a mean error of about 5−7 cm^{-1}, whatever the probed modes.

Acknowledgment. The authors thank M. Mons and his group for fruitful and stimulating discussions for the assignment of the structures of the peptides.

Supporting Information Available: List of the peptides used as training set, table of the average of error ϵ for asymmetric and symmetric NH_2 stretches for all methods with a unique scaling factor, and table of specific local scaling factors when distinction between symmetric and asymmetric NH_2 stretches is established. This material is available free of charge via the Internet at http://pubs.acs.org.

References and Notes

(1) de Vries, M. S.; Hobza, P. *Annu. Rev. Phys. Chem.* **2007**, *58*, 585.
(2) Dian, B. C.; Longarte, A.; Mercier, S.; Evans, D. A.; Wales, D. J.; Zwier, T. S. *J. Chem. Phys.* **2002**, *117*, 10688.
(3) Chin, W.; Mons, M.; Dognon, J. P.; Mirasol, R.; Chass, G.; Dimicoli, I.; Piuzzi, F.; Butz, P.; Tardivel, B.; Compagnon, I.; von Helden, G.; Meijer, G. *J. Phys. Chem. A* **2005**, *109*, 5281.
(4) Inokuchi, Y.; Kobayashi, Y.; Ito, T.; Ebata, T. *J. Phys. Chem. A* **2007**, *111*, 3209.
(5) Stearns, J. A.; Mercier, S.; Seaiby, C.; Guidi, M.; Boyarkin, O. V.; Rizzo, T. R. *J. Am. Chem. Soc.* **2007**, *129*, 11814.
(6) Hunig, I.; Kleinermanns, K. *Phys. Chem. Chem. Phys.* **2004**, *6*, 2650.
(7) Abo-Riziq, A. G.; Crews, B.; Bushnell, J. E.; Callahan, M. P.; De Vries, M. S. *Mol. Phys.* **2005**, *103*, 1491.
(8) Reha, D.; Valdes, H.; Vondrasek, J.; Hobza, P.; Abu-Riziq, A.; Crews, B.; de Vries, M. S. *Chemistry-a European Journal* **2005**, *11*, 6803.
(9) Haber, T.; Seefeld, K.; Engler, G.; Grimme, S.; Kleinermanns, K. *Phys. Chem. Chem. Phys.* **2008**, *10*, 2844.
(10) Unterberg, C.; Gerlach, A.; Schrader, T.; Gerhards, M. *J. Chem. Phys.* **2003**, *118*, 8296.
(11) Gerhards, M.; Unterberg, C.; Gerlach, A.; Jansen, A. *Phys. Chem. Chem. Phys.* **2004**, *6*, 2682.
(12) Fricke, H.; Funk, A.; Schrader, T.; Gerhards, M. *J. Am. Chem. Soc.* **2008**, *130*, 4692.
(13) Chin, W.; Dognon, J. P.; Piuzzi, F.; Tardivel, B.; Dimicoli, I.; Mons, M. *J. Am. Chem. Soc.* **2005**, *127*, 707.
(14) Chin, W.; Mons, M.; Dognon, J. P.; Piuzzi, F.; Tardivel, B.; Dimicoli, I. *Phys. Chem. Chem. Phys.* **2004**, *6*, 2700.
(15) Chin, W.; Piuzzi, F.; Dognon, J. P.; Dimicoli, I.; Mons, M. *J. Chem. Phys.* **2005**, *123*, 084301.
(16) Brenner, V.; Piuzzi, F.; Dimicoli, I.; Tardivel, B.; Mons, M. *J. Phys. Chem. A* **2007**, *111*, 7347.
(17) Stearns, J. A.; Boyarkin, O. V.; Rizzo, T. R. *J. Am. Chem. Soc.* **2007**, *129*, 13820.
(18) Gerhards, M.; Unterberg, C.; Gerlach, A. *Phys. Chem. Chem. Phys.* **2002**, *4*, 5563.
(19) Fricke, H.; Gerlach, A.; Gerhards, M. *Phys. Chem. Chem. Phys.* **2006**, *8*, 1660.
(20) Bakker, J. M.; Plutzer, C.; Hunig, I.; Haber, T.; Compagnon, I.; von Helden, G.; Meijer, G.; Kleinermanns, K. *ChemPhysChem* **2005**, *6*, 120.
(21) Chin, W.; Dognon, J. P.; Canuel, C.; Piuzzi, F.; Dimicoli, I.; Mons, M.; Compagnon, I.; von Helden, G.; Meijer, G. *J. Chem. Phys.* **2005**, *122*, 054317.
(22) Gregoire, G.; Gaigeot, M. P.; Marinica, D. C.; Lemaire, J.; Schermann, J. P.; Desfrancois, C. *Phys. Chem. Chem. Phys.* **2007**, *9*, 3082.
(23) Vaden, T. D.; Gowers, S. A. N.; de Boer, T.; Steill, J. D.; Oomens, J.; Snoek, L. C. *J. Am. Chem. Soc.* **2008**, *130*, 14640.
(24) Carcabal, P.; Kroemer, R. T.; Snoek, L. C.; Simons, J. P.; Bakker, J. M.; Compagnon, I.; Meijer, G.; von Helden, G. *Phys. Chem. Chem. Phys.* **2004**, *6*, 4546.

(25) Fricke, H.; Gerlach, A.; Unterberg, C.; Rzepecki, P.; Schrader, T.; Gerhards, M. *Phys. Chem. Chem. Phys.* **2004**, *6*, 4636.
(26) Mercier, S. R.; Boyarkin, O. V.; Kamariotis, A.; Guglielmi, M.; Tavernelli, I.; Cascella, M.; Rothlisberger, U.; Rizzo, T. R. *J. Am. Chem. Soc.* **2006**, *128*, 16938.
(27) Abo-Riziq, A.; Bushnell, J. E.; Crews, B.; Callahan, M.; Grace, L.; De Vries, M. S. *Chem. Phys. Lett.* **2006**, *431*, 227.
(28) Abo-Riziq, A.; Crews, B. O.; Callahan, M. P.; Grace, L.; de Vries, M. S. *Angew. Chem., Int. Ed.* **2006**, *45*, 5166.
(29) Chin, W.; Piuzzi, F.; Dimicoli, I.; Mons, M. *Phys. Chem. Chem. Phys.* **2006**, *8*, 1033.
(30) Brause, R.; Fricke, H.; Gerhards, M.; Weinkauf, R.; Kleinermanns, K. *Chem. Phys.* **2006**, *327*, 43.
(31) Carcabal, P.; Jockusch, R. A.; Hunig, I.; Snoek, L. C.; Kroemer, R. T.; Davis, B. G.; Gamblin, D. P.; Compagnon, I.; Oomens, J.; Simons, J. P. *J. Am. Chem. Soc.* **2005**, *127*, 11414.
(32) Carney, J. R.; Zwier, T. S. *J. Phys. Chem. A* **1999**, *103*, 9943.
(33) Snoek, L. C.; Kroemer, R. T.; Simons, J. P. *Phys. Chem. Chem. Phys.* **2002**, *4*, 2130.
(34) Cerny, J.; Hobza, P. *Phys. Chem. Chem. Phys.* **2007**, *9*, 5291.
(35) Zhao, Y.; Truhlar, D. G. *J. Chem. Theory Comput.* **2006**, *2*, 1009.
(36) Zhao, Y.; Truhlar, D. G. *Acc. Chem. Res.* **2008**, *41*, 157.
(37) Grimme, S. *J. Comput. Chem.* **2004**, *25*, 1463.
(38) Jurecka, P.; Cerny, J.; Hobza, P.; Salahub, D. R. *J. Comput. Chem.* **2007**, *28*, 555.
(39) Schwabe, T.; Grimme, S. *Acc. Chem. Res.* **2008**, *41*, 569.
(40) Grimme, S. *J. Comput. Chem.* **2006**, *27*, 1787.
(41) Cerny, J.; Jurecka, P.; Hobza, P.; Valdes, H. *J. Phys. Chem. A* **2007**, *111*, 1146.
(42) Morgado, C.; Vincent, M. A.; Hillier, I. H.; Shan, X. *Phys. Chem. Chem. Phys.* **2007**, *9*, 448.
(43) Jurecka, P.; Nachtigall, P.; Hobza, P. *Phys. Chem. Chem. Phys.* **2001**, *3*, 4578.
(44) Frontera, A.; Quinonero, D.; Garau, C.; Costa, A.; Ballester, P.; Deya, P. M. *J. Phys. Chem. A* **2006**, *110*, 9307.
(45) Riley, K. E.; Hobza, P. *J. Phys. Chem. A* **2007**, *111*, 8257.
(46) Trygubenko, S. A.; Bogdan, T. V.; Rueda, M.; Orozco, M.; Luque, F. J.; Sponer, J.; Slavicek, P.; Hobza, P. *Phys. Chem. Chem. Phys.* **2002**, *4*, 4192.
(47) Hanus, M.; Ryjacek, F.; Kabelac, M.; Kubar, T.; Bogdan, T. V.; Trygubenko, S. A.; Hobza, P. *J. Am. Chem. Soc.* **2003**, *125*, 7678.
(48) Jurecka, P.; Hobza, P. *J. Am. Chem. Soc.* **2003**, *125*, 15608.
(49) Hanus, M.; Kabelac, M.; Rejnek, J.; Ryjacek, F.; Hobza, P. *J. Phys. Chem. B* **2004**, *108*, 2087.
(50) Valdes, H.; Klusak, V.; Pitonak, M.; Exner, O.; Stary, I.; Hobza, P.; Rulisek, L. *J. Comput. Chem.* **2008**, *29*, 861.
(51) Valdes, H.; Pluhackova, K.; Pitonak, M.; Rezac, J.; Hobza, P. *Phys. Chem. Chem. Phys.* **2008**, *10*, 2747.
(52) Crews, B.; Abo-Riziq, A.; Grace, L.; Callahan, M.; Kabelac, M.; Hobza, P.; de Vries, M. S. *Phys. Chem. Chem. Phys.* **2005**, *7*, 3015.
(53) Callahan, M. P.; Crews, B.; Abo-Riziq, A.; Grace, L.; de Vries, M. S.; Gengeliczki, Z.; Holmes, T. M.; Hill, G. A. *Phys. Chem. Chem. Phys.* **2007**, *9*, 4587.
(54) Abo-Riziq, A.; Crews, B. O.; Compagnon, I.; Oomens, J.; Meijer, G.; Von Helden, G.; Kabelac, M.; Hobza, P.; de Vries, M. S. *J. Phys. Chem. A* **2007**, *111*, 7529.
(55) Neugebauer, J.; Hess, B. A. *J. Chem. Phys.* **2003**, *118*, 7215.
(56) Carbonniere, P.; Barone, V. *Chem. Phys. Lett.* **2004**, *399*, 226.
(57) Barone, V.; Festa, G.; Grandi, A.; Rega, N.; Sanna, N. *Chem. Phys. Lett.* **2004**, *388*, 279.
(58) Brauer, B.; Chaban, G. M.; Gerber, R. B. *Phys. Chem. Chem. Phys.* **2004**, *6*, 2543.
(59) Wang, J. P.; Hochstrasser, R. M. *J. Phys. Chem. B* **2006**, *110*, 3798.
(60) Barone, V. *J. Phys. Chem. A* **2004**, *108*, 4146.
(61) Bouteiller, Y.; Gillet, J. C.; Gregoire, G.; Schermann, J. P. *J. Phys. Chem. A* **2008**, *112*, 11656.
(62) Ahlrichs, R.; Bar, M.; Haser, M.; Horn, H.; Kolmel, C. *Chem. Phys. Lett.* **1989**, *162*, 165.
(63) Weigend, F.; Haser, M. *Theor. Chem. Acc.* **1997**, *97*, 331.
(64) Schafer, A.; Horn, H.; Ahlrichs, R. *J. Chem. Phys.* **1992**, *97*, 2571.
(65) Schafer, A.; Huber, C.; Ahlrichs, R. *J. Chem. Phys.* **1994**, *100*, 5829.
(66) Dunning, T. H. *J. Chem. Phys.* **1989**, *90*, 1007.
(67) Weigend, F.; Haser, M.; Patzelt, H.; Ahlrichs, R. *Chem. Phys. Lett.* **1998**, *294*, 143.
(68) Weigend, F.; Kohn, A.; Hattig, C. *J. Chem. Phys.* **2002**, *116*, 3175.
(69) Lee, C. T.; Yang, W. T.; Parr, R. G. *Phys. Rev. B* **1988**, *37*, 785.
(70) Becke, A. D. *Phys. Rev. A* **1988**, *38*, 3098.
(71) Weigend, F. *Phys. Chem. Chem. Phys.* **2006**, *8*, 1057.
(72) Frisch, M. J.; Pople, J. A.; Binkley, J. S. *J. Chem. Phys.* **1984**, *80*, 3265.
(73) Ahlrichs, R.; Furche, F.; Grimme, S. *Chem. Phys. Lett.* **2000**, *325*, 317.
(74) Handy, N. C.; Murray, C. W.; Amos, R. D. *J. Phys. Chem.* **1993**, *97*, 4392.
(75) Eichkorn, K.; Weigend, F.; Treutler, O.; Ahlrichs, R. *Theor. Chem. Acc.* **1997**, *97*, 119.
(76) Hattig, C.; Hellweg, A.; Kohn, A. *Phys. Chem. Chem. Phys.* **2006**, *8*, 1159.
(77) Kolar, M.; Hobza, P. *J. Phys. Chem. A* **2007**, *111*, 5851.
(78) Busker, M.; Svartsov, Y. N.; Haber, T.; Kleinermanns, K. *Chem. Phys. Lett.* **2009**, *467*, 255.
(79) Correia, C. F.; Clavaguera, C.; Erlekam, U.; Scuderi, D.; Ohanessian, G. *ChemPhysChem* **2008**, *9*, 2564.
(80) Chin, W.; Piuzzi, F.; Dognon, J. P.; Dimicoli, L.; Tardivel, B.; Mons, M. *J. Am. Chem. Soc.* **2005**, *127*, 11900.

JP901570R